

Two-component electron fluid in underdoped high- T_c cuprate superconductors

J. G. STOREY¹ and J. L. TALLON²

¹ *MacDiarmid Institute for Advanced Materials and Nanotechnology - School of Chemical and Physical Sciences, Victoria University of Wellington, P.O. Box 500, Wellington, New Zealand.*

² *MacDiarmid Institute - Industrial Research Ltd., P.O. Box 31310, Lower Hutt, New Zealand.*

PACS 74.25.Jb – Electronic structure
 PACS 74.72.-h – Cuprate superconductors
 PACS 74.25.nj – Nuclear magnetic resonance
 PACS 74.62.Fj – Effects of pressure

Abstract – Evidence from NMR of a two-component spin system in cuprate high- T_c superconductors is shown to be paralleled by similar evidence from the electronic entropy so that a two-component quasiparticle fluid is implicated. We propose that this two-component scenario is restricted to the optimal and underdoped regimes and arises from the upper and lower branches of the reconstructed energy-momentum dispersion proposed by Yang, Rice and Zhang (YRZ) to describe the pseudogap. We calculate the spin susceptibility within the YRZ formalism and show that the doping and temperature dependence reproduces the experimental data for the cuprates.

From the electronic entropy we present evidence for a two-component electron fluid in underdoped high- T_c cuprates matching similar evidence from NMR [1–3]. We then show that this two-component behavior probably arises from Fermi surface reconstruction and the associated band-splitting that occurs due to pseudogap correlations. We illustrate this using the model proposed by Yang, Rice and Zhang (YRZ) [4]. Implicit in this interpretation is the prediction that single-component behavior is recovered in the overdoped region where the pseudogap closes around $p \approx 0.19$ holes/Cu.

Hole-doped HTS, in their overdoped state, possess a large Fermi surface [5–7] enclosing $(1 + p)$ carriers where p is the doped hole concentration residing largely on in-plane oxygen orbitals and the “1” arises from the unpaired electrons residing on the Cu sites. This naively suggests a two-component electron system. However, Zhang and Rice [8] showed that the doped holes form a local singlet state with the hole on the Cu $3d_{x^2-y^2}$ orbital, the so-called Zhang-Rice singlet. It was suggested that the singlet binding energy was so large that the oxygen $2p$ holes do not contribute to the spin susceptibility thus resulting in a single-component spin scenario. This situation has been considered long-established starting from Takigawa *et al.* [9], who showed that the ^{17}O and ^{63}Cu Knight shifts, $^{17}K(T)$ and $^{63}K(T)$ respectively, for un-

derdoped $\text{YBa}_2\text{Cu}_3\text{O}_{7-\delta}$ exhibit an identical temperature dependence. Subsequent ^{89}Y NMR studies confirmed the same T -dependence in $^{89}K(T)$ [10] adding further weight to the single-component scenario.

However, this **single-component** picture was recently questioned by Haase *et al* [1–3]. In order to eliminate the Meissner term in the spin shift they constructed a term G_\perp by subtracting the Knight shift for the apical oxygen with field perpendicular to the c -axis from that for the planar Cu shift, and similarly G_\parallel for field parallel to the c -axis. Thus,

$$\begin{aligned} G_\perp(T) &= {}^{63,\perp}K(T) - {}^{17,A,\perp}K(T), \\ G_\parallel(T) &= {}^{17,P,\parallel}K(T) - {}^{17,A,\parallel}K(T), \end{aligned} \quad (1)$$

where the superscript A refers to the apical oxygen while the superscript P refers to planar oxygen.

These authors showed that $G_\perp(T)$ displayed a T -independent Pauli-like metallic susceptibility, while $G_\parallel(T)$ displayed a strongly T -dependent susceptibility consistent with a gapped normal-state spectrum. By constructing a two-component ansatz:

$$\begin{aligned} G_\perp(T) &= c_{11}\chi_1 + c_{12}\chi_2, \\ G_\parallel(T) &= c_{21}\chi_1 + c_{22}\chi_2, \end{aligned} \quad (2)$$

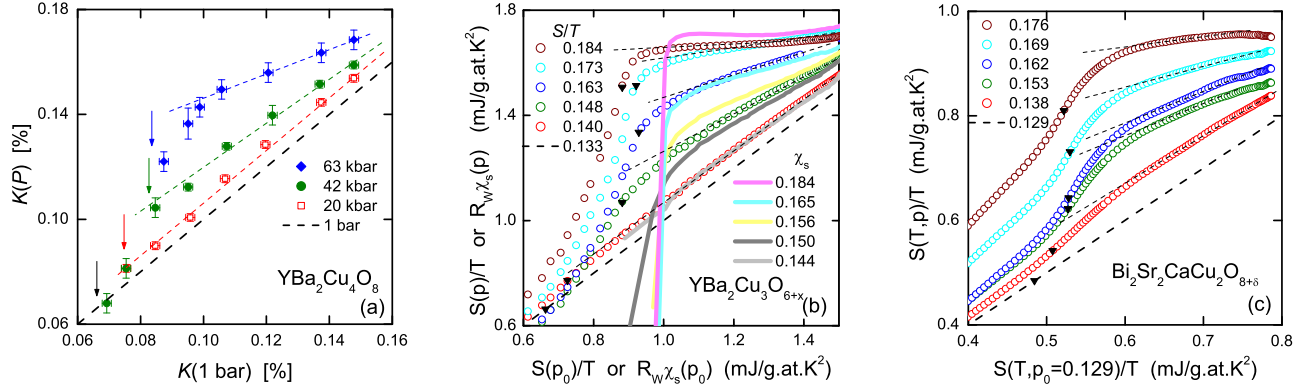


Fig. 1: (Color online) (a) Reproduced from ref. [9]: the Knight shift, $K(P)$, for $\text{YBa}_2\text{Cu}_4\text{O}_8$ at $P = 20, 42$ and 63 kbar plotted vs $K(1 \text{ bar})$ where T is the implicit variable. Arrows indicate T_c . Above the range of SC fluctuations $K(P)$ is linear in $K(1 \text{ bar})$. (b) An analogous plot of $S(T, p)/T$ for $\text{YBa}_2\text{Cu}_3\text{O}_{6+x}$ plotted vs $S(T, p_0 = 0.133)/T$ for $x = 0.76, 0.80, 0.87, 0.92$ and 0.97 (open circles). The corresponding p values are listed. Also shown is $R_W\chi_s(T, p)$ vs $R_W\chi_s(T, p_0 = 0.135)$, expressed in entropy units (solid curves). (c) $S(T, p)/T$ for $\text{Bi}_2\text{Sr}_2\text{CaCu}_2\text{O}_{8+\delta}$ plotted vs $S(T, p_0 = 0.129)/T$ for the listed p -values.

where χ_1 and χ_2 are the two putative uniform susceptibilities, Haase *et al.* [1] showed that $\chi_1(T)$ has a characteristic pseudogap-like T -dependence, falling steadily towards zero with reducing T , while $\chi_2(T)$ has a constant Pauli-like behavior and only falls to zero below T_c with the opening of the superconducting (SC) energy gap.

In introducing χ_1 and χ_2 Haase *et al.* took a lead from Johnston [11] who, from static bulk measurements, inferred a two-component susceptibility of the form $\chi(p, T) = \chi_1(p, T) + \chi_2(p)$ where χ_2 is a function of doping only. However, the features he sought to explain arise naturally from the presence of the van Hove singularity (vHs) in the overdoped region which ensures an overall increasing density of states across most of the phase diagram (as reflected in the $\chi_2(p)$ term). A single-component susceptibility fully accounts for the complete evolution of $^{89}\text{K}_s$ across the underdoped and overdoped regions in $\text{Y}_{0.8}\text{Ca}_{0.2}\text{Ba}_2\text{Cu}_3\text{O}_{7-\delta}$ [12] provided the full ARPES derived dispersion is utilized, including the vHs. It requires a differential measurement, as in Eq.(1), to expose the true underlying two-component behavior.

To make the problem more specific we consider the most recent study from the Haase group [3], which also supports the two-component picture. In this they carried out high-pressure diamond-anvil NMR measurements on $\text{YBa}_2\text{Cu}_4\text{O}_8$ to 63 kbar. Pressure, P , acts dominantly, though not exclusively, to increase the doping by transferring holes from the Cu_2O_2 chains to the CuO_2 planes. Thus one typically observes a pressure-induced decrease in thermoelectric power [13] consistent with an increase in hole concentration, p , resulting in a pressure-induced increase in T_c on the underdoped side and a decrease in T_c on the overdoped side [14]. (That the effect of pressure is not *merely* to increase the hole concentration is evident from the fact that the maximum T_c is increased from approx 93 K at ambient pressure to approximately

107 K at a pressure of about 7 GPa [15]). Consistent with this, Meissner *et al.* [3] observed $^{17}\text{K}(T)$ to progress from a strongly T -dependent behavior under ambient pressure, typical of a pseudogapped underdoped cuprate, towards a nearly T -independent behavior at a pressure of 63 kbar, more typical of an optimally-doped cuprate. By plotting $^{17}\text{K}(T, P)$ versus $^{17}\text{K}(T, P = 1 \text{ bar})$ for $P = 20, 42$ and 63 kbar with T as the implicit variable they obtained a linear relation that showed a characteristic progression with increasing P . This plot is reproduced in Fig. 1(a).

The authors draw attention to the fact that well above T_c there is a linear region that for the lowest doping extends down almost to T_c . They model this linear behavior within a two-component scenario.

Firstly we wish to point out that identical behavior is seen in the electronic entropy, $S(T)$, thus indicating that it is not just the spin system that exhibits two components but the total quasiparticle ensemble.

For a nearly free-electron system the spin susceptibility, χ_s and S/T are related via the Wilson ratio, R_W :

$$R_W\chi_s(T) = S(T)/T. \quad (3)$$

Accordingly, the open circles in Fig. 1(b) and (c) show $S(T, p)/T$ versus $S(T, p_0)/T$ (where T is the implicit variable) for $\text{YBa}_2\text{Cu}_3\text{O}_{6+x}$ (b) and for $\text{Bi}_2\text{Sr}_2\text{CaCu}_2\text{O}_{8+\delta}$ (c). We choose $p_0 = 0.133$ for the former and $p_0 = 0.129$ for the latter, which are close to the zero-pressure doping state of $\text{YBa}_2\text{Cu}_4\text{O}_8$, $p_0 \approx 0.13$. The same generic behavior also occurs in plots of $S(T, p)/T$ versus $S(T, p_0)/T$ for $\text{Y}_{0.8}\text{Ca}_{0.2}\text{Ba}_2\text{Cu}_3\text{O}_{6+x}$ (not shown). The correspondence between $K(P)$ and $S(p)/T$ is remarkable.

Assuming the major effect of pressure is to increase doping and letting α be the thermopower, then $(\partial\alpha/\partial P)_{T=290} = -0.075 \mu\text{V K}^{-1}\text{kbar}^{-1}$ [13]. Using the thermopower correlation with doping $(\partial\alpha/\partial p)_{T=290} =$

$-134\mu\text{V K}^{-1}\text{hole}^{-1}$ [16] one finds $(\partial p/\partial P) = 5.6 \times 10^{-4}$ holes/kbar. Thus the doping states of $\text{YBa}_2\text{Cu}_4\text{O}_8$ at 20, 42 and 63 kbar are 0.141, 0.154 and 0.165 holes/Cu. Visually the red, green and blue data sets in Fig. 1(a) correspond closely to the red, green and blue data sets in Fig. 1(b) and so should be at roughly the same doping states. This is indeed the case where in Fig. 1(b) the dopings are seen to be 0.140, 0.148 and 0.163 holes/Cu.

Moreover, we show that the correspondence between χ_s and S/T is in excellent quantitative agreement with Eq. 3. The solid curves in Fig. 1(b) show values of $\chi_s(T, p)$ versus $\chi_s(T, p_0 = 0.135)$ expressed in entropy units using the Wilson ratio for nearly-free electrons $R_W^0 = (\pi^2/3)(k_B/\mu_B)^2$. We use the bulk susceptibility χ_s data of Cooper and Loram [16]. One can see that the correspondence between χ_s and S/T is not just qualitative but quantitative. These plots reveal precisely the same magnitudes as S/T and the same breakaway from linear behavior sets in well above T_c due to strong SC fluctuations [17]. (Note that below T_c the diamagnetism leads to different behavior from S/T). We thus conclude that there is in fact a two-component *quasiparticle system*, not just a two-component *spin system*.

We now turn to our central thesis that this generic behavior, seen in both the spin susceptibility and the entropy, arises from band splitting that occurs when the Fermi surface reconstructs due to competing orders such as a CDW, SDW or short-range AF correlations. We illustrate this within the YRZ scenario where the electron self-energy term $E_g^2(\mathbf{k})/(\omega + \xi_{\mathbf{k}}^0)$ reconstructs the $E(\mathbf{k})$ dispersion into upper and lower branches which yield our two-component quasiparticle ensemble. Here $\xi_{\mathbf{k}}^0 = -2t(p)(\cos k_x + \cos k_y)$ is the nearest-neighbor term in the tight-binding $E(\mathbf{k})$ dispersion. The coherent part of the electron Green's function is given by:

$$G(\mathbf{k}, \omega, p) = g_t(p) \left[\omega - \xi_{\mathbf{k}} - \frac{E_g^2(\mathbf{k})}{\omega + \xi_{\mathbf{k}}^0} \right]^{-1}. \quad (4)$$

where $\xi_{\mathbf{k}} = -2t(p)(\cos k_x + \cos k_y) - 4t'(p)\cos k_x \cos k_y - 2t''(p)(\cos 2k_x + \cos 2k_y) - \mu_p(p)$ is the tight-binding dispersion to third-nearest neighbors, and $E_g(\mathbf{k}) = \frac{1}{2}E_g^0(p)(\cos k_x - \cos k_y)$ is the pseudogap with doping dependence $E_g^0(p) = 3t_0(0.2 - p)$, while for $p > 0.2$ we have $E_g^0(p) = 0$. (This means the pseudogap closes at $p = 0.2$ however we have extensively shown this to occur at slightly lower doping $p = 0.19$ [18]. Here we retain the value 0.2 to remain consistent with YRZ). The chemical potential $\mu_p(p)$ is chosen according to the Luttinger sum rule. The doping dependent coefficients are given by $t(p) = g_t(p)t_0 + (3/8)g_s(p)J\chi$, $t'(p) = g_t(p)t'_0$ and $t''(p) = g_t(p)t''_0$, where $g_t(p) = 2p/(1+p)$ and $g_s(p) = 4/(1+p)^2$ are the Gutzwiller factors. The bare parameters $t'/t_0 = -0.3$, $t''/t_0 = 0.2$, $J/t_0 = 1/3$ and $\chi = 0.338$ are the same as used previously [4].

Equation 4 can be re-written as

$$G(\mathbf{k}, \omega, p) = \sum_{\alpha=\pm} \frac{g_t(p)W_{\mathbf{k}}^{\alpha}(p)}{\omega - E_{\mathbf{k}}^{\alpha}(p)}, \quad (5)$$

where the energy-momentum dispersion is reconstructed by the pseudogap into upper and lower branches

$$E_{\mathbf{k}}^{\pm} = \frac{1}{2}(\xi_{\mathbf{k}} - \xi_{\mathbf{k}}^0) \pm \sqrt{\left(\frac{\xi_{\mathbf{k}} + \xi_{\mathbf{k}}^0}{2}\right)^2 + E_g^2(\mathbf{k})}, \quad (6)$$

which are weighted by

$$W_{\mathbf{k}}^{\pm} = \frac{1}{2} \left[1 \pm \frac{(\xi_{\mathbf{k}} + \xi_{\mathbf{k}}^0)/2}{\sqrt{[(\xi_{\mathbf{k}} + \xi_{\mathbf{k}}^0)/2]^2 + E_g^2(\mathbf{k})}} \right]. \quad (7)$$

The spectral function is given by

$$A(\mathbf{k}, \omega, p) = \sum_{\alpha=\pm} g_t(p)W_{\mathbf{k}}^{\alpha}\delta(\omega - E_{\mathbf{k}}^{\alpha}), \quad (8)$$

from which the density of states can be calculated

$$N(\omega) = \sum_{\mathbf{k}} A(\mathbf{k}, \omega). \quad (9)$$

Finally, the spin susceptibility is given by

$$\chi_s = 2\mu_B^2 \int \left(-\frac{\partial f}{\partial \omega} \right) N(\omega) d\omega. \quad (10)$$

Figure 2(a) shows the partial densities of states (PDOS) for $p = 0.14$ and 0.16 calculated from the upper and lower branches of the reconstructed dispersion given by Eq. 6. The PDOS of the lower branch is quasi-linear across the Fermi level ($\omega = 0$) resulting in a roughly T -independent contribution to the susceptibility at low doping, shown in Fig. 2(b) by the solid curves. For dopings below about 0.18, the PDOS of the upper branch lies above the Fermi level resulting in a gapped spectrum. With decreasing doping the upper PDOS is pushed further from $\omega = 0$, producing a T -dependent contribution to χ that is characteristic of the pseudogap state, shown in Fig. 2(b) by the dashed curves.

The two sets of susceptibilities shown by the dashed and solid curves in Fig. 2(b) are to be directly compared with the functions $\chi_1(T)$ and $\chi_2(T)$, respectively, reported by Haase *et al.*, [1, 2]. They reveal the same qualitative behavior but there are points of difference, primarily in their relative magnitudes where, at high temperature, the lower-branch susceptibility is more than three times the magnitude of the upper-branch susceptibility. By contrast, Haase *et al.* find χ_2 exceeds χ_1 by around 50% at 300 K. We return to this discrepancy below.

In order to compare directly with the pressure- and doping-dependent data shown in Figure 1 we plot in Fig. 2(c) the sum of the susceptibilities (from the upper and lower branches) as a function of the susceptibility sum for $p = 0.13$, with T as the implicit variable.

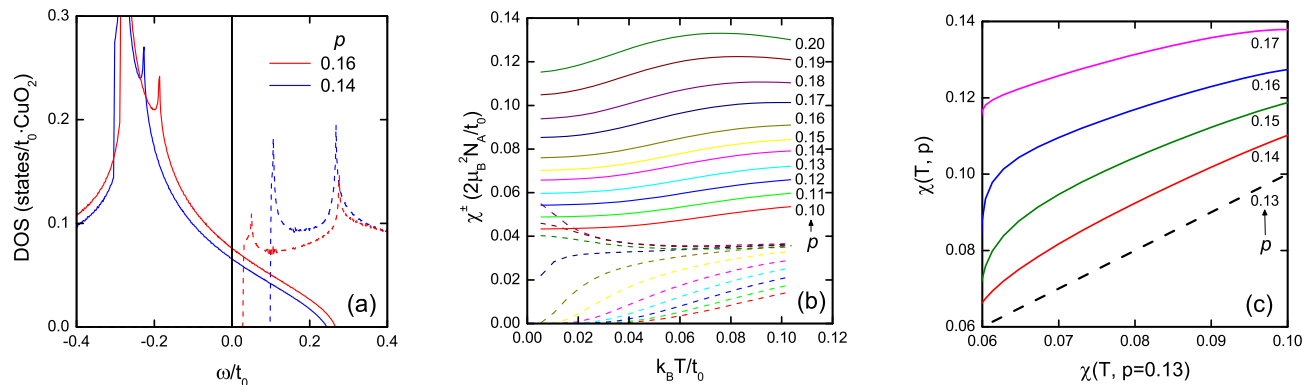


Fig. 2: (Color online) (a) Partial density of states calculated from the lower (solid) and upper (dashed) branches of the YRZ reconstructed dispersion. (b) Susceptibility calculated from the lower (solid) and upper (dashed) partial density of states. (c) Total $\chi_s(T, p)$ plotted versus $\chi_s(T, p_0 = 0.13)$ where T is the implicit variable (units of χ are the same as in (b)).

The qualitative features seen in the normal-state Knight shift (Fig. 1(a)) and electronic entropy (Figs. 1(b) & (c)) are reproduced in detail. In particular, the high- T downturn seen for $p = 0.17$ reflects the proximity of the vHs. The same downturn is seen in the $\text{Bi}_2\text{Sr}_2\text{CaCu}_2\text{O}_{8+\delta}$ data (Fig. 1(c)) where the vHs indeed lies nearby [19] in the moderately overdoped region, whereas it is not evident in the data for $\text{YBa}_2\text{Cu}_3\text{O}_{7-\delta}$ (Fig. 1(b)) where the vHs is known to lie in the more deeply overdoped region.

We are however left with two remaining questions: (i) why does $G_\perp(T)$ reflect more the lower branch susceptibility while $G_\parallel(T)$ reflects more the upper branch susceptibility? And (ii) there is the question, mentioned above, of the relative magnitudes of the two susceptibilities. We suggest these have a common origin, as follows:

The apical oxygen is coupled to the planar copper and oxygen orbitals via the Cu 4s orbital [20]. This introduces matrix elements that weight the \mathbf{k} -space sums, minimizing the contribution along the zone diagonals and maximizing contributions at the $(\pi, 0)$ zone boundaries. This clearly will diminish the contribution to the susceptibility from the lower branch, effectively reducing the magnitude of the coefficients c_{12} and c_{22} . As a consequence the relative contributions of χ_1 and χ_2 to $G_\perp(T)$ and $G_\parallel(T)$ differ, with $G_\perp(T)$ dominated more by χ_2 . The c -axis hopping matrix is $t_\perp(\mathbf{k}) = t_\perp^0 \mu_{\mathbf{k}}^2$ where $\mu_{\mathbf{k}} = 0.5 \omega_{\mathbf{k}} (\cos k_x - \cos k_y)$. We find this does indeed bring the magnitudes of χ_1 and χ_2 closer together for lower doping but not so much at higher doping close to where the pseudogap closes. We await a more rigorous treatment of the precise interaction of the apical nucleus with the two global spin susceptibilities.

In conclusion, we show that the entropy term $S(T)/T$ displays the same doping evolution as the pressure-dependent Knight shift, thus indicating that the two-component electronic behavior resides in the quasiparticle spectrum and not just in the spin spectrum. We then show that the essential features of the two-component system are likely to arise from band splitting due to zone-folding

effects as described e.g. by the Yang-Rice-Zhang model for the pseudogap. The pseudogap-like susceptibility χ_1 inferred by Haase *et al.* arises from the upper branch and the Pauli-like χ_2 arises from the lower branch. If correct then it follows that single-component electronic behavior will be recovered when the pseudogap closes. Measurements of G_\perp and G_\parallel will then help settle the still contentious issue as to whether the pseudogap closes abruptly, both above the SC dome and below it at a putative quantum critical point at $p \approx 0.19$.

REFERENCES

- [1] HAASE J., SLICHTER C. P. and WILLIAMS G. V. M., *J. Phys.: Condens. Matter*, **20** (2008) 434227.
- [2] HAASE J., SLICHTER C. P. and WILLIAMS G. V. M., *J. Phys.: Condens. Matter*, **21** (2009) 455702.
- [3] MEISSNER T., GOH S. K., HAASE J., WILLIAMS G. V. M. and LITTLEWOOD P. B., *Phys. Rev. B*, **83** (2011) 220517(R).
- [4] YANG K. Y., RICE T. M. and ZHANG F. C., *Phys. Rev. B*, **73** (2006) 174501.
- [5] HUSSEY N. E., ABDEL-JAWAD M., CARRINGTON A., MACKENZIE A. P. and BALICAS L., *Nature*, **425** (2003) 814.
- [6] PLATÉ M., MOTTERSHEAD J. D. F., ELFIMOV I. S., PEETS D. C., LIANG R., BONN D. A., HARDY W. N., CHIUZBAIAN S., FALUB M., SHI M., PATTHEY L. and DAMASCELLI A., *Phys. Rev. Lett.*, **95** (2005) 077001.
- [7] VIGNOLLE B., CARRINGTON A., COOPER R. A., FRENCH M. M. J., MACKENZIE A. P., JAUDET C., VIGNOLLES D., PROUST C. and HUSSEY N. E., *Nature*, **455** (2008) 952.
- [8] ZHANG F. C. and RICE T. M., *Phys. Rev. B*, **37** (1988) 3759.
- [9] TAKIGAWA M., REYES A. P., HAMMEL P. C., THOMPSON J. D., HEFFNER R. H., FISK Z. and OTT K. C., *Phys. Rev. B*, **43** (1991) 247.

- [10] ALLOUL H., OHNO T. and MENDELS P., *Phys. Rev. Lett.*, **63** (1989) 1700.
- [11] JOHNSTON D. C., *Phys. Rev. Lett.*, **62** (1989) 957.
- [12] STOREY J. G., TALLON J. L. and WILLIAMS G. V. M., *Phys. Rev. B*, **76** (2007) 174522.
- [13] ZHOU J. S. and GOODENOUGH J. B., *Phys. Rev. B*, **53** (1996) R11976.
- [14] SCHLACHTER S. I., FIETZ W. H., GRUBE K., WOLF T., OBST B., SCHWEISS P. and KLÄSER M., *Physica C*, **328** (1999) 1.
- [15] SCHOLTZ J. J., VAN EENIGE E. N., WIJNGAARDEN R. J. and GRIESSEN R., *Phys. Rev. B*, **45** (1992) 3077.
- [16] COOPER J. R. and LORAM J. W., *J. Phys. I France*, **6** (1996) 2237.
- [17] TALLON J. L., STOREY J. G. and LORAM J. L., *Phys. Rev. B*, **83** (2011) 092502.
- [18] TALLON J. L. and LORAM J. W., *Physica C*, **349** (2001) 53.
- [19] KAMINSKI A., ROSENKRANZ S., FRETWELL H. M., NORMAN M. R., RANDEIRA M., CAMPUZANO J. C., PARK J. M., LI Z. Z. and RAFFY H., *Phys. Rev. B*, **73** (2006) 174511.
- [20] XIANG T. and WHEATLEY J. M., *Phys. Rev. Lett.*, **77** (1996) 4632.